JACS
JOURNAL OF THE AMERICAN CHEMICAL SOCIETY

COMMUNICATION

pubs.acs.org/JACS

Dual Lithium Insertion and Conversion Mechanisms in a Titanium-Based Mixed-Anion Nanocomposite

Damien Dambournet,*[,†] Karena W. Chapman,*[,‡] Peter J. Chupas,[‡] Rex E. Gerald, II,[†] Nicolas Penin,[§] Christine Labrugere,[§] Alain Demourgues,[§] Alain Tressaud,[§] and Khalil Amine[†]

[†]Chemical Sciences and Engineering Division and [‡]X-ray Science Division, Advanced Photon Source, Argonne National Laboratory, Argonne, Illinois 60439, United States

[§]Institut de Chimie de la Matière Condensée de Bordeaux-CNRS, Université Bordeaux, 33607 Pessac Cedex, France

Supporting Information

ABSTRACT: The electrochemical reaction of lithium with a vacancy-containing titanium hydroxyfluoride was studied. On the basis of pair distribution function analysis, NMR, and X-ray photoelectron spectroscopy, we propose that the material undergoes partitioning upon initial discharge to form a nanostructured composite containing crystalline Li_xTiO_2, surrounded by a Ti^0 and LiF layer. The Ti^0 is reoxidized upon reversible charging to an amorphous TiF_3 phase via a conversion reaction. The crystalline Li_xTiO_2 is involved in an insertion reaction. The resulting composite electrode, Ti^0-LiF/Li_xTiO_2 ⇔ TiF_3/ Li_yTiO_2, allows reaction of more than one Li per Ti, providing a route to higher capacities while improving the energy efficiency compared to pure conversion chemistries.

A challenge in expanding lithium-ion battery technology from portable electronic devices to electric vehicles is realizing the high-energy storage densities needed. The energy density of conventional electrode materials is limited by their intercalation chemistry, with only up to a single electron transferred per redox-active metal ion. New electrodes, based on multielectron redox processes, can overcome this limitation.[1,2] Rather than inserting Li, these materials undergo reversible reduction to form metal nanoparticles M^0 and binary Li compounds: $M^{z+}X_y + zLi^+ + ze^- \rightleftarrows M^0 + yLi_{z/y}X$.[3−6] This was first documented in binary transition metal oxides[3] and subsequently in other systems.[4−6] The multicomponent, often nanoscale nature of conversion reactions can be challenging to characterize. Advanced structure probes must be combined to completely understand these reactions.[7]

Titanium compounds are attractive electric energy storage candidates owing to their versatile redox chemistry, relative abundance, and nontoxic nature.[8] While thermodynamic considerations allow for conversion of TiO_2, in practice, electrochemical activity is limited to insertion involving the Ti^{4+}/Ti^{3+} redox couple.[9] Due to their electronegativity, fluoride ligands increase the output voltage, facilitating reduction and, accordingly, conversion. However, a large voltage hysteresis compromises performance.[5,10] Mixed-anion oxy- or hydroxyfluorides offer an attractive compromise, with reduced polarization, tunable redox potentials, and improved cycle stability.[11]

Here we investigate the electrochemical reactions of a mixed-anion system derived from vacancy-containing titanium hydroxyfluoride ($Ti_{0.75}\square_{0.25}F_{1.5}(OH)_{1.5}$).[12] The reversible capacity reported here was less than that expected for full conversion but greater than that for intercalation alone. Analysis of high-energy X-ray scattering data using the pair distribution function (PDF) method and complementary X-ray photoelectron spectroscopy (XPS) and NMR measurements indicates that, unlike other mixed anion systems,[13] titanium hydroxyfluoride is not the electroactive component responsible for the reversible energy storage. Instead, the initial discharge (lithiation) process induces an irreversible partitioning of the hydroxyfluoride into oxide- and fluoride-rich phases. These components are involved in parallel, reversible intercalation and conversion processes, respectively.

Nanoscale titanium hydroxyfluoride (80 nm) was prepared by microwave-assisted hydrothermal methods.[14] This hydroxyfluoride is related to cubic $TiOF_2$, with corner-sharing Ti octahedra; however, substitution of O^{2-} by OH under these synthetic conditions produces cationic vacancies disordered throughout the lattice. The electrochemistry was tested by cycling against Li^0. For structure characterization, data were collected for the starting material and materials recovered in various states of discharge and charge. High-energy X-ray scattering data, suitable for PDF analysis, were collected at 11-ID-B at the Advanced Photon Source to probe the redox-active titanium phase(s). The PDF provides local and intermediate-range structural insights as a histogram of all atom−atom distances within a material, independent of long-range order. Complementary NMR and XPS were used to probe the chemical environment of the weakly X-ray-scattering Li ions and to identify phases at the particle surface.

The electrochemical activity of the system during the first two discharge/charge cycles is shown in Figure 1. There are two plateaus during the initial discharge, indicative of structural transitions. The very small plateau at 1.3 V is likely associated with the Li-induced cubic-to-rhombohedral transition known for ReO_3 phases such as $TiOF_2$ (see Supporting Information (SI)).[15] The larger plateau at 0.8 V is associated with a capacity of ∼700 mA h g^{-1} (or 2.35 Li per formula unit). The absence of this plateau in the reverse or subsequent cycles indicates that the accompanying structural change (phase or microstructure) is irreversible.

The initial discharge, to 0.05 V, spanned a capacity of 875 mA h g^{-1} (or 2.94 Li). The large, irreversible component results in a

Received: May 10, 2011
Published: August 02, 2011

lower capacity charge cycle. In the second and successive cycles (see SI), the reversible capacity stabilized to 400 mA h g^{-1} at an average 1.3 V. This reversible behavior involves ~1.3 Li per formula unit, beyond that attributable to intercalation alone, with an operating voltage between those for intercalation (~1.7 V for TiO_2) and conversion (~1.2 V for TiF_3).

The structural changes associated with the discharge/charge reactions were probed using X-ray scattering methods (Figure 2). While the sample appeared to amorphize irreversibly during the initial discharge, based on measurements using Cu Kα radiation (λ = 1.54 Å), high-energy X-ray (λ = 0.21 Å) scattering measurements showed that Bragg reflections were retained for all samples. The most pronounced changes in the high-energy diffraction and PDF data were evident between the initial and cycled materials. By contrast, only minor changes were evident in the PDFs and Bragg reflections upon further charge or discharge. The broad reflections in the high-energy X-ray data for the discharged and charged samples suggest a cubic rock-salt phase. Re-examination of the laboratory X-ray data revealed weak features at corresponding 2θ values of 43.9° and 64° (or $Q \approx$ 3.1 and 4.3 $Å^{-1}$, see SI).

Refinement of a structure model based on the cubic rock-salt phase, Li_xTiO_2, provided an excellent fit to the PDF data ($Fm\bar{3}m$, a = 4.13 Å, $R_w \approx$ 11.8%, Figure 3).[16] Rock-salt phases are found in many intercalation reactions.[17] This phase is formed by edge-sharing Ti octahedra. The PDF for the charged material contained similar features at larger distances. These were broadened compared to those of the discharged material, indicating increased disorder upon delithiation. At short distance, some differences in local coordination geometry were evident. Application of the optimized Li_xTiO_2 model to the data for the charged material, refining atomic displacement and scale parameters, yielded an excellent fit to the intermediate- and long-range data ($R_w \approx$ 13.7%, r-range 8−20 Å) but could not reproduce the intensity and position of features at low r ($R_w \approx$ 41%, 1.5−20 Å). The residual to the limited r-range fit (Figure 3) suggested the presence of a second phase with no long-range order (e.g., an amorphous phase). The features associated with this second, poorly ordered phase are consistent with corner-sharing polyhedra, although they clearly differ from those of the pristine material (Figure 2c). This could be modeled by an amorphous phase based on TiF_3 (see SI).[18] Refinement of a two-phase model to all data (1.5−20 Å) yielded a good fit ($R_w \approx$ 19.4%), with an estimated mole ratio of 1.4 Li_xTiO_2:1 TiF_3.

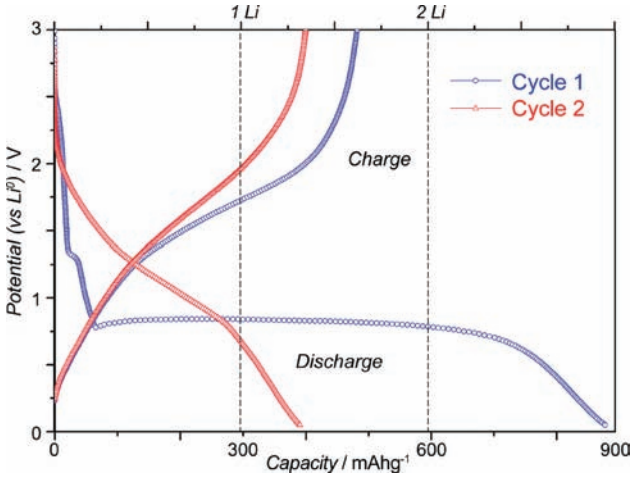

Figure 1. Voltage profile obtained upon discharge/charge of titanium hydroxyfluoride, cycled between 0.05 and 3 V at 100 mA g^{-1}.

Surface-sensitive XPS methods were used to identify surface species for samples recovered from discharged and charged states (Figure 4). The fully discharged sample was pretreated with mild Ar sputtering (60 s) to remove possible surface contaminants. During sample discharge, the peaks associated with Ti 2p progressively disappear, while peaks associated with Li 1s and F 1s species increase. This indicates the formation of LiF, extruded as a film on the particle surface, with a characteristic F 1s signal at 685.5 eV and Li 1s signal centered at 56.1 eV.[19] A minor contribution to the Li 1s signal at 54.1 eV is characteristic of Li_2O.[20] The intensity of the LiF peaks decreases upon recharging, indicating that LiF is consumed upon oxidation (a fluorination reaction).

To probe the active Li environments and verify their involvement in the reversible electrochemistry, ^{7}Li MAS NMR spectroscopy measurements were performed. The data indicate that ionic Li, with features centered at 0 ppm, exists in two distinct environments associated with Li_xTiO_2 and LiF phases (see SI). The intensity of each contribution depends on the state of charge/discharge, with signals attenuating upon charging, confirming the involvement of both species in the reversible cycling reaction.

The data suggest that the structural transition during the large plateau on initial discharge involves partitioning of the anions in the hydroxyfluoride, to extrude LiF and leave Li_xTiO_2. The hydrogen from the hydroxyfluoride may form H_2 or react with

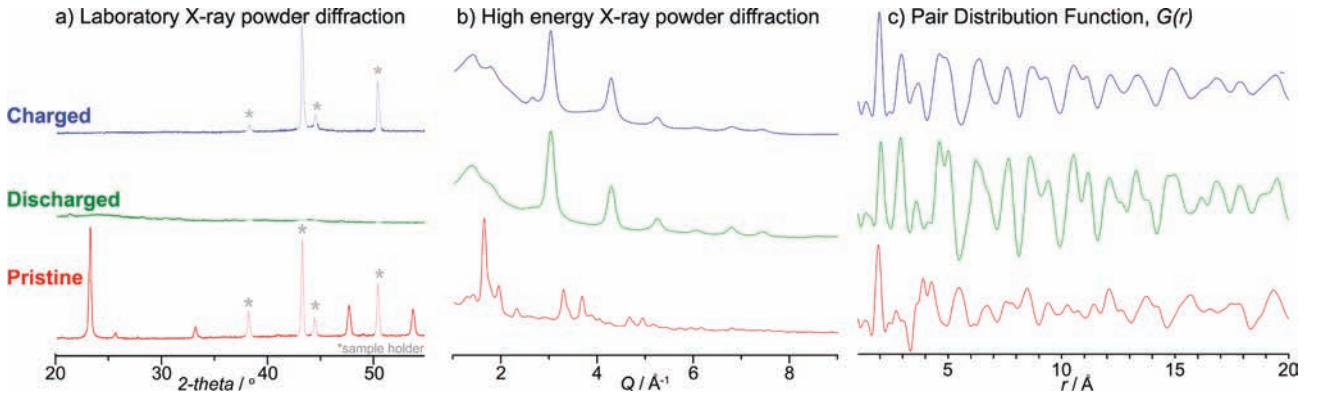

Figure 2. X-ray scattering data for the initial (red), fully discharged (green), and charged (blue) materials, as measured using (a) a laboratory-based X-ray source (Cu Kα radiation, λ = 1.54 Å), (b) high-energy X-rays (λ = 0.21 Å), and (c) the corresponding PDFs.

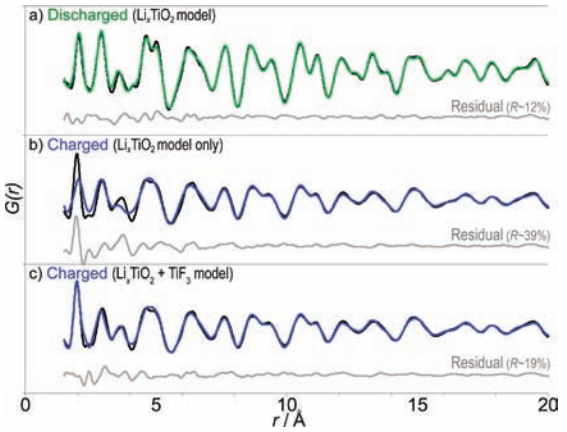

Figure 3. PDFs for the discharged (green) and charged (blue) materials, the models fit to the data (black), and residuals to the fit (gray).

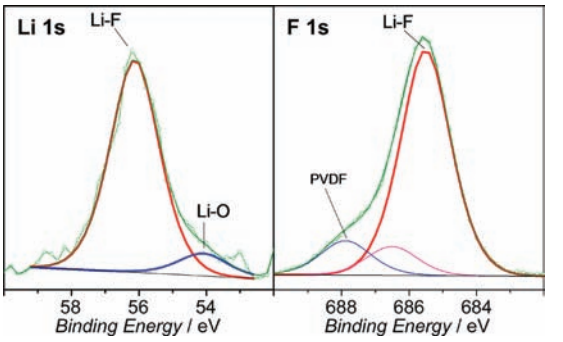

Figure 4. XPS spectra of the discharged sample (Li and F 1s core).

the electrolyte. Li_xTiO_2, a phase which is present in both the charged and discharged states, is involved in a Li intercalation mechanism. As for other TiO_2 phases,[21] the titanium oxide framework connectivity remains unchanged throughout the intercalation/de-intercalation processes, without transforming to a more stable polymorph of TiO_2 at very low Li levels. Although metallic Ti was not observed in the recovered samples, based on our understanding of conversion mechanisms, the concomitant formation of TiF_3 and decomposition of LiF upon charging suggests that metallic Ti forms according to the reaction $Ti^0 + 3LiF \leftrightarrow TiF_3 + 3Li^+ + 3e^-$. Any metallic Ti formed by reduction of a highly disordered TiF_3 may be highly reactive and may be reoxidized (by trace O_2, H_2O, LiOH) during the sample recovery, possibly forming the cubic rock-salt TiO_2 phase.

Partitioning of anions has been observed in other hydroxyfluorides, where the pure oxide and fluoride are more stable that the mixed-anion phase.[22] While fits to the PDF are largely insensitive to O/F substitution, anion partitioning is supported by several observations. First, substitution of F into Li_xTiO_2 is unlikely due to the unfavorable energetics of edge-sharing F. Also, the Li_xTiO_2:TiF_3 ratio of 1.4:1, suggested by the PDF analysis, is close to the 1.5:1 ratio expected for complete partitioning, without OH condensation or LiOH formation. Further, based on the theoretical capacities of Li_xTiO_2 and TiF_3 (335 and 770 mA h g^{-1}), the mole ratio of 1.4:1 corresponds to a capacity of 390 mA h g^{-1}, close to the observed reversible capacity of the composite (400 mA h g^{-1}).[23]

The apparent difference between laboratory-based and high-energy X-ray experiments—amorphous vs crystalline—can be attributed to the different penetration of the X-rays into the sample and the sample microstructure. The titanium-containing component strongly absorbs the low-energy Cu Kα radiation, and, as such, the X-rays only penetrate the surface of the sample.[23] In contrast, high-energy X-rays are highly penetrating and probe the full sample volume. This suggests that an amorphous titanium-containing layer (amorphous TiF_3/Ti^0) may largely surround the crystalline core (Li_xTiO_2), obscuring the crystalline component from the low-penetrating Cu Kα radiation. This type of core−shell-like architecture, with an amorphous phase surrounding a crystalline component, has been observed in other systems.[22,25]

The present study indicates that the initial titanium hydroxyfluoride is not part of the reversible electrochemical reaction and capacity. Instead, a nanostructured composite is formed, Ti^0-$LiF/Li_xTiO_2 \leftrightarrow TiF_3/Li_yTiO_2$, with electrochemical activity involving parallel intercalation and conversion mechanisms. This permits a greater average number of Li to be exchanged per redox-active center compared to that for intercalation alone. During the initial discharge, lithium insertion induces a cubic-to-rhombohedral transition in the titanium hydroxyfluoride, followed by an irreversible partitioning of the fluoro and oxo anions. This first-order transition involves extrusion of LiF, and likely formation of metallic Ti, to stabilize an edge-sharing Li_xTiO_2 phase. The metallic Ti is proposed to reoxidize during the ensuing charging, to produce an amorphous TiF_3 phase via a conversion reaction that consumes LiF. This amorphous TiF_3 forms as a layer surrounding the crystalline rock-salt Li_xTiO_2 phase from which Li is concomitantly extracted (de-intercalation), thereby increasing local structure distortions. Subsequent discharge/charge cycles involve insertion/removal of Li in the Li_xTiO_2 core and conversion of the amorphous shell from TiF_3 to Ti metal. The amorphous nature of TiF_3 is consistent with the lack of a plateau during reversible cycling.[25] These parallel insertion and conversion mechanisms may operate in a previously studied titanium oxyfluoride.[27,28]

In summary, we have applied PDF, XPS, and NMR to understand the reactions of lithium with titanium hydroxyfluoride. The identification of electrochemically active phases demonstrates the value of the PDF method for studying electrode materials. Although rational targeting of the conversion reaction was found to be complex, PDF methods can improve our understanding, paving the way for new discoveries. It is important to note that diffraction studies using Cu Kα radiation can be misleading if they are not interpreted with care: for transition metal systems, including those where amorphization is suspected, the use of higher energy X-rays is advisable. The nanocomposite generated here from partitioning of a mixed-anion phase displays parallel mechanisms involving both lithium intercalation and conversion chemistries. This dual mechanism offers routes to higher capacities than can be achieved with pure intercalation chemistries while improving the energy efficiency of pure conversion chemistries; the composite has a polarization of 0.5 V, compared to 1 V for TiF_3. Ongoing efforts are focused on (1) evaluating the impact of composition on the electrochemical properties in these mixed-anion systems, where the O:F ratio can be controlled synthetically, to provide a unique means to tailor electrochemical behavior (e.g., reversible capacity, energy efficiency), and (2) in situ PDF studies during electrochemical cycling, to provide more detailed insight into the reactions and reactive species.

■ ASSOCIATED CONTENT

Supporting Information. Details about sample preparation, experimental procedures, and analysis. This material is available free of charge via the Internet at http://pubs.acs.org.

■ AUTHOR INFORMATION

Corresponding Author
damien_dambournet@yahoo.fr; chapmank@aps.anl.gov

■ ACKNOWLEDGMENT

This work was funded, in part, by the U.S. Department of Energy (DOE), FreedomCAR, and Vehicle Technologies Office. Work done at Argonne and use of the Advanced Photon Source, an Office of Science User Facility operated for the U.S. DOE Office of Science by Argonne National Laboratory, were supported by the U.S. DOE under Contract No. DE-AC02-06CH11357. We acknowledge support from the French Centre National de la Recherche Scientifique (CNRS) and discussions with I. Belharouak, N. Karan, and M. Balasubramanian.

■ REFERENCES

(1) Armand, M.; Tarascon, J.-M. *Nature* **2008**, *451*, 652.
(2) Gao, X.-P; Yang, H.-X. *Energy Environ. Sci.* **2010**, *3*, 174.
(3) Poizot, P.; Laruelle, S.; Grugeon, S.; Dupont, L.; Tarascon, J. M. *Nature* **2000**, *407*, 496.
(4) Cabana, J.; Monconduit, L.; Larcher, D.; Palacin, M. R. *Adv. Mater.* **2010**, *22*, E170.
(5) Li, H.; Richter, G.; Maier, J. *Adv. Mater.* **2003**, *15*, 736.
(6) Badway, F.; Cosandey, F.; Pereira, N.; Amatucci, G. G. *J. Electrochem. Soc.* **2003**, *150*, A1318.
(7) Yamakawa, N.; Jiang, M.; Key, B.; Grey, C. P. *J. Am. Chem. Soc.* **2009**, *131*, 10525.
(8) Deng, D.; Kim, M. G.; Lee, J. Y.; Cho, J. *Energy Environ. Sci.* **2009**, *2*, 818.
(9) Li, H.; Balaya, P.; Maier, J. *J. Electrochem. Soc.* **2004**, *151*, A1878.
(10) Oumellal, Y.; Rougier, A.; Nazri, G. A.; Tarascon, J. M.; Aymard, L. *Nat. Mater.* **2008**, *7*, 916.
(11) Pereira, N.; Badway, F.; Wartelsky, M.; Gunn, S.; Amatucci., G. G. *J. Electrochem. Soc.* **2009**, *156*, A407.
(12) Demourgues, A.; Penin, N.; Durand, E.; Weill, F.; Dambournet, D.; Viadere, N.; Tressaud, A. *Chem. Mater.* **2009**, *21*, 1275.
(13) Bervas, M.; Klein, L. C.; Amatucci, G. G. *J. Electrochem. Soc.* **2006**, *153*, A159–A170.
(14) *Functionalized Inorganic Fluorides: Synthesis, Characterizations & Properties of Nanostructured Solids*; Tressaud, A., Ed.; Wiley-Blackwell: Chichester, 2010; Chapters 2 and 8.
(15) Murphy, D. W; Greenblatt, M.; Cava, R. J.; Zahurak, S. M. *Solid State Ionics* **1981**, *5*, 327.
(16) Lecerf, A. *Ann. Chim.* **1962**, 513.
(17) Pralong, V. *Prog. Solid State Chem.* **2009**, *37*, 262.
(18) Hoppe, R.; Becker, S. *Z. Anorg. Allg. Chem.* **1989**, *568*, 126.
(19) Lu, Y. C.; Mansour, A. N.; Yabuuchi, N.; Shao-Horn, Y. *Chem. Mater.* **2009**, *21*, 4408.
(20) Dedryvere, R.; Laruelle, S.; Grugeon, S; Poizot, P; Gonbeau, D; Tarascon, J. M. *Chem. Mater.* **2004**, *16*, 1056.
(21) Dambournet, D.; Chapman, K. W.; Koudriachova, M. V.; Chupas, P. J.; Belharouak, I; Amine, K. *Inorg. Chem.* **2011**, 5855.
(22) Dambournet, D.; Demourgues, A.; Martineau, C.; Majimel, J.; Feist, M.; Legein, C.; Buzaré, J.-Y.; Fayon, F.; Tressaud, A. *J. Phys. Chem. C* **2008**, *112*, 12374.
(23) Interfacial energy storage phenomena may contribute to the additional capacity observed: Yu, X. Q.; Sun, J. P.; Tang, K.; Li, H.; Huang, X. J.; Dupont, L.; Maier, J. *Phys. Chem. Chem. Phys.* **2009**, *11*, 9497.
(24) *Fundamentals of Powder Diffraction and Structural Characterization of Materials*Pecharsky, V. K., Zavalij, P. Y., Eds.; Kluwer: Boston, 2003.
(25) Carenco, S.; Le Goff, X. F.; Shi, J.; Roiban, L.; Ersen, O.; Boissière, C.; Sanchez, C.; Mézailles, N. *Chem. Mater.* **2011**, *23*, 2270.
(26) Delmer, O; Balaya, P.; Kienle, L.; Maier, J *Adv. Mater.* **2008**, *20*, 501.
(27) Reddy, M. V.; Madhavi, S.; Subba Rao, G. V.; Chowdari., B. V. R. *J. Power Sources* **2006**, *162*, 1312.
(28) A previous study[27] of titanium oxyfluoride showed high capacities (~400 mA h g^{-1}); however, an apparent amorphization of the material, based on diffraction studies using Cu Kα radiation, impeded further understanding of this reaction. While the authors dismissed the possibility of conversion, close inspection of their diffraction data reveals weak features at $2\theta \approx 44$ and 64°, consistent with Li_xTiO_2 formation. We propose that a similar Ti^0-$LiF/Li_xTiO_2 \leftrightarrow TiF_3/Li_yTiO_2$ nanocomposite is formed.